State Space Decoupling Approach for Feedback Controller Design of Switching Converters

E. de C. Gomes*, L. A. de S. Ribeiro**, J. V. M. Caracas**, S. Y. C. Catunda**, R. D. Lorenz***
* IFMA, Av. Getúlio Vargas no. 4, Monte Castelo, 65020-000, São Luís - Ma, Brazil
** UFMA/IEE, Av. dos Portugueses, s/n, Campus Universitário do Bacanga, 65080-040, São Luís - Ma, Brazil
*** University of Wisconsin - Madison, WEMPEC, 1513 University Ave, Madison, WI 53706

***Abstract*-- This paper derives a new approach for analyzing dc-dc converters for feedback control design. The control-to-output voltage transfer function of the converters, usually predicted by averaging models, and the classical feedback control techniques are replaced by the state space average state block diagram analysis. These state block diagrams are obtained for state space averaging matrixes of the converters combined with their continuous conduction mode differential equations. This technique yields first order control transfer functions allowing easier synthesis of controllers. The resulting controllers demonstrate good transient response compared to voltage controllers based on k-factor approach. The structure is easy implement with relevant applications in integrated circuit manufacturing and industrial environment.**

***Index Terms*-- DC-DC converter, K-factor design, State Space Control, Voltage Controllers.**

I. INTRODUCTION

Dc-dc converters with pulse width modulation are time varying, non-linear circuits that are usually modeled by small-signal averaging models. The state-space representation combined with the average technique of modeling results in the state-space averaging modeling [1]. The advantage of this approach is the inclusion of LC output filter in modeling process. The *PWM Switch* is a methodology similar to linear amplifier circuit that the basic idea is modeling only the switching elements of the power stage to obtain an equivalent circuit of these elements called *PWM Switch Model* [2]. These models were developed for continuous and discontinuous conduction operation, and the continuous conduction mode (CCM) model is often used for control design.

After having formed the small signal representation of the power stage [3], the feedback controller to regulate the output voltage can be designed with the following objectives: zero steady state error, fast response to changes in the input voltage and the output load, low overshoot, and noise immunity.

Voltage mode control and current mode control are two traditional control techniques [4]. The transient response of voltage mode control exhibits good noise immunity. However, its dynamic behavior is governed by complex poles. Current mode control improves the transient response characteristics by feeding back the inductor current. Two types of control have been established: 1) Peak current mode control that is popular and has been used for decades; 2) average current-mode control. The drawback of the former is its inherent instability when duty ratio is greater than one half and the need a stabilizing ramp to overcome the problem. The advantages of average current-mode control, such as the ability to control the average inductor current and the improvement of noise immunity, no additional stability ramp circuit is included in [4]. Both peak current-mode control and average current-mode control structures are more difficult and more expensive to implement compared to voltage mode control. Furthermore, the classical definition of bandwidth is not clear in the design of these controllers [5], [6].

The averaging models predict a control-to-output voltage transfer function with a complex pole pair (resonance) whose analysis for design of a suitable controller become a challenge based on a trial-and-error procedure. The k-factor is a simple and effective method for dealing with plants having complex dynamic behavior. It is a mathematical tool that eliminates the trial-and-error process to tune the controller as is normally made in classical controllers designed with the well-known root locus method. To use this method, stability criteria must be reviewed since the concepts of phase boost and bandwidth are treated as fundamental variables to obtain stability [7].

Mixed voltage–current mode control has already been developed and it has given better control performance than the standard PI voltage control approaches [8],[9]. It is shown in [8],[9] that using a state block diagram to represent the dynamic behavior of a system, one can readily identify how the state variables are cross-coupled and how it is possible to decouple, i.e. cancel, the effects of these variables on each other. Such state space decoupling controllers become easier to synthesize and they can be completely designed based on their bandwidth or zero/pole locations. With state space decoupling control the dynamic response of buck converter presents fast load response with small dynamic deviations from the desired steady state output value. State space decoupling control will exhibit quasi total input variation immunity [10].

The subject of this paper is propose a systematic state space decoupling control structure, with easy implementation, moderate cost and satisfactory dynamic responses, based on bandwidth. To design the controllers a state block diagram of the converters was derived. Comparisons with k-factor voltage mode control approach will be made and the results will be commented later.

This work was supported by the Federal University of Maranhão, Brasil.

II. Power Stage and Small Signal Analysis of Basic Second Order Converters

The buck converter power stage with pulse width modulator is depicted in Fig. 1. During normal operation the switch Q is repeatedly switched on and off with the on and off times governed by the control circuit. This switch action causes a train of pulses at point A which is filtered by the LC output filter to produce a dc output voltage. R_C and R_L are parasitic elements representing the equivalent series resistances of the capacitor and inductor, respectively.

The duration of the ON and OFF states in continuous operation mode is given by (1) and (2), where D is the duty cycle set by the control circuit, and T_s is the time of one complete switch cycle.

$$T_{on} = DT_s \tag{1}$$

$$T_{off} = (1-D)T_s \tag{2}$$

Applying the principles of steady-state converter analysis [4] and assuming that switch, diode and inductor resistance voltage drops are small enough to be ignored, the voltage conversion relationship for output voltage V_O can be determined by (3), where V_{IN} is the input voltage of the buck converter.

$$V_O = DV_{IN} \tag{3}$$

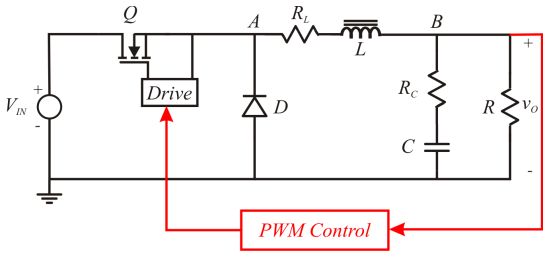

Fig. 1. Buck converter power stage schematic.

The steps to do small signal analysis of the system for small changes around the dc steady state operating point to obtain the buck converter transfer function using state-space averaging approach are detailed in [3]. These steps are summarized as:

(a) State-variable description for each circuit state;

$$\dot{X} = A_t X + B_t V_{IN} \tag{4}$$

(b) Averaging the state-variable description using the duty ratio;

$$\dot{X} = [A_1 d + A_2(1-d)]X + [B_1 d + B_2(1-d)]V_{IN} \tag{5}$$

$$v_o = [C_1 d + C_2(1-d)]X \tag{6}$$

(c) Introducing small ac perturbations and separation into ac and dc components;

$$x = X + \tilde{x} \tag{7}$$

$$v_o = V_o + \widetilde{v_o} \tag{8}$$

$$d = D + \tilde{d} \tag{9}$$

$$v_{in} = V_{IN} + \widetilde{v_{in}} \tag{10}$$

(d) Determination of the transfer function, and transformation into complex domain.

$$\frac{V_o}{V_{IN}} = -CA^{-1}B \tag{11}$$

$$\frac{\widetilde{v_o}}{\tilde{d}} = C[sI - A]^{-1}[(A_1 - A_2)X + (B_1 - B_2)V_{IN}] + (C_1 - C_2)X \tag{12}$$

Utilizing the four steps above, the control-to-output voltage transfer function of buck converter can be obtained and expressed by (13).

$$G_{PS}(s) = V_{IN} \cdot \frac{R}{R + R_L} \cdot \frac{1 + sR_C C}{As^2 + Bs + 1} \tag{13}$$

where

$$A = LC\frac{R + R_c}{R + R_L} \text{ and } B = C\left(R_c + \frac{RR_L}{R + R_L}\right) + \frac{L}{R + R_L}$$

Repeating the previous steps for boost and buck-boost converters, we obtain the control-to-output voltage transfer functions presented in Table 1.

TABLE I
CONTROL-TO-OUTPUT VOLTAGE TRANSFER FUNCTIONS OF (A) BOOST AND (B) BUCK-BOOST CONVERTER.

$G_{PS}(s) = \frac{V_{IN}}{(1-D)^2} \frac{\left(1 - \frac{L_e}{R}s\right)(1 + R_C Cs)}{L_e C\left[s^2 + \left(\frac{R_C}{L_e(1-D)} + \frac{1}{RC}\right)s + \frac{1}{L_e C}\right]}$	(a)
$\frac{\widetilde{v_o}(s)}{\tilde{d}(s)} = \frac{V_{IN}}{(1-D)^2} \frac{\left(1 - \frac{DL_e}{R}s\right)(1 + R_C Cs)}{L_e C\left[s^2 + \left(\frac{R_C}{L_e(1-D)} + \frac{1}{RC}\right)s + \frac{1}{L_e C}\right]}$	(b)

With $L_e = \frac{L}{(1-D)^2}$

III. The K-Factor Approach

One of the tools used to design controllers for dc-dc converters is the k-factor. This approach will be used as a metric to compare the results proposed in this paper. The type-3 k-factor controller is often used for compensation of buck and boost converters due to its ability to provide the phase boost needed to obtain the desired phase margin and crossover frequency for the closed loop controller [7]. The schematic diagram and transfer function of the type-3 k-factor compensator are shown in Fig. 2, and (14).

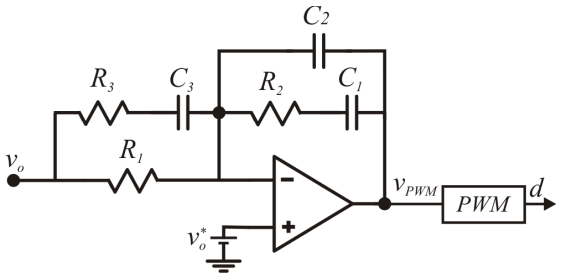

Fig. 2. A type-3 k-factor compensator.

$$\frac{V_o(s)}{V_i(s)} = -\frac{(1 + sR_2C_1)[1 + sC_3(R_1 + R_3)]}{sR_1(C_1 + C_2 + sR_2C_1C_2)(1 + sR_3C_3)} \tag{14}$$

The type-3 k-factor compensator transfer function (14) can also be written as in (15).

$$G_c = \frac{\frac{\omega_{co}}{A_{co}K}\left(\frac{\sqrt{K}}{\omega_{co}}s+1\right)^2}{s\left(\frac{s}{\sqrt{K}\omega_{co}}+1\right)^2} \quad (15)$$

where ω_{co} is the desired crossover frequency, K is the pole and zero frequencies control factor and it can be adjusted depending on the phase boost (θ_{boost}) required to make the phase compensation. Given the desired phase margin PM and the crossover frequency, the phase boost that the compensator can provide is given by (16) and the K value is calculated by (17).

$$\theta_{boost} = PM - 90° - \theta_{power-stage} \quad (16)$$

$$K = tg^2\left(\frac{\theta_{boost}}{4} + 45°\right) \quad (17)$$

An important constraint required in the k-factor design procedure is that the crossover frequency has to be less than one-fourth of the switching frequency to avoid large signal instability. Thus, given R_1, the other components can be calculated as shown in Table II.

TABLE II
CONTROLLER COMPONENTS DESIGN USING K-FACTOR APPROACH

$k_c = G_c\frac{\omega_z}{\theta_{boost}}$	$C_2 = \frac{2\omega_z}{k_c\omega_p R_1}$
$C_1 = C_2\left(\frac{\omega_p}{\omega_z}-1\right)$	$R_2 = \frac{1}{\omega_z C_1}$
$R_3 = \frac{R_1}{\left(\frac{\omega_p}{\omega_z}-1\right)}$	$C_3 = \frac{1}{\omega_p R_3}$

IV. A STATE SPACE DECOUPLING APPROACH

Another way to design a controller for a system is to look at its state block diagram instead of its transfer function. The state block diagram shows explicitly how the state variables are coupled, and this is important when designing a controller exploring the physical features of the system.

A. State Block Diagrams of Basic 2nd Order Converters

To obtain the average model, state block diagram of buck converter, we must use the state space average matrixes generated by (5) and (6) for each state (on and off) of the power switch in CCM [10]. The differential equations written from these matrixes are given by (18), (19) and (20).

$$L\frac{d\tilde{\imath}_L}{dt} = -\frac{RR_C + RR_L + R_LR_C}{R+R_C}\tilde{\imath}_L - \frac{R}{R+R_C}\tilde{v}_C + \tilde{d}V_{IN} \quad (18)$$

$$C\frac{d\tilde{v}_C}{dt} = \frac{R}{R+R_C}i_L - \frac{1}{R+R_C}\tilde{v}_C \quad (19)$$

$$\widetilde{v_o} = \frac{RR_C}{R+R_C}\tilde{\imath}_L + \frac{R}{R+R_C}\tilde{v}_C \quad (20)$$

Defining the parameters and gains in Table III, the buck average state block diagram can be depicted as shown in Fig. 3.

TABLE III
PARAMETERS OF THE BUCK AVERAGE MODEL, STATE BLOCK DIAGRAM

$R_1 = \frac{RR_C + RR_L + R_CR_L}{R+R_C}$	$G_1 = \frac{R}{R+R_C}$
$R_2 = \frac{RR_C}{R+R_C}$	$R_3 = R + R_C$

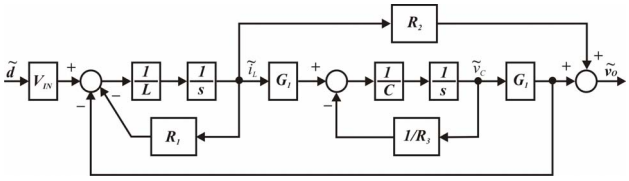

Fig. 3. The average model, state block diagram of buck converter.

Using the same procedure, and defining the parameters and gain showed in Table IV, the average model, state block diagrams of boost and buck-boost converters can be obtained as presented in Fig. 4. For buck–boost converters, a block with the duty cycle D must be placed before the input showed in Fig. 4. The same procedure can be used to derive the state block diagram of any converter. For example, the state block diagram of the forward converter is similar to that depicted in Fig. 3, except that the turn ratio of the transformer must be included.

TABLE IV
PARAMETERS OF THE BOOST AND BUCK-BOOST AVERAGE MODEL, STATE BLOCK DIAGRAMS

$G_2 = \frac{R[R(1-D)+R_C]}{RR_L + R_LR_C + RR_C(1-D) + R^2(1-D)^2}$	
$G_3 = \frac{R}{R+R_C}(1-D)$	$R_4 = R_L + \frac{RR_C}{R+R_C}(1-D)$
$R_5 = \frac{RR_C}{R+R_C}(1-D)$	$R_6 = R(1-D) + R_C$

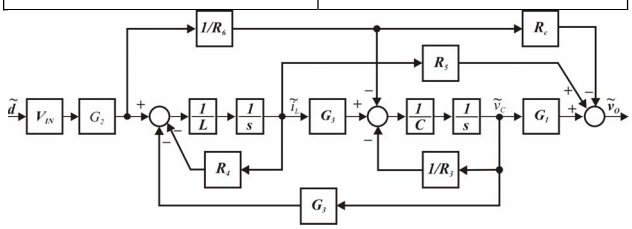

Fig. 4. The average model, state block diagram of boost converter.

B. State Space Decoupling

State space decoupling is a technique that uses state space feedback to decouple the cross-coupling among states, resulting, in general, systems with better dynamic properties [8], [9], [10]. It will be used in this paper in the design of controllers for dc-dc converters.

As an example, by analyzing the state block diagram of the buck converter (see Fig. 3) it is clear that the capacitor voltage and inductor current states are cross-coupled. If it is possible to measure the capacitor voltage, this cross-coupling could be eliminated. However, it is impossible to exactly decouple this cross-coupling because the only variable that can be measured is the output voltage, instead of the true capacitor voltage. Applying a positive feedback as depicted in Fig. 5, it is still possible to decouple, i.e. cancel, the cross-coupling

between the voltage and current states. The system poles, initially complex, moves to the real axis, located at $p_1 = -\frac{R_L}{L}$, and $p_2 = -\frac{1}{C(R+R_3)}$. In general R_L (equivalent series resistance of the inductor) is a small value (parasitic element), and the dominant pole (p_1), related to the inductor current, moved to a position closer to the origin of the complex plane. This is because of the link between $\tilde{\imath}_L$and $\tilde{v}_o$ through the resistor R_2. This is an interesting feature of doing the decoupling by using the output voltage, and emphasizes the potential use of a simple proportional controller for current, especially for the cases where $R_L \cong 0$. Furthermore, the current and voltage states can be analyzed independently, as depicted in the decoupled state block diagram of Fig. 6.

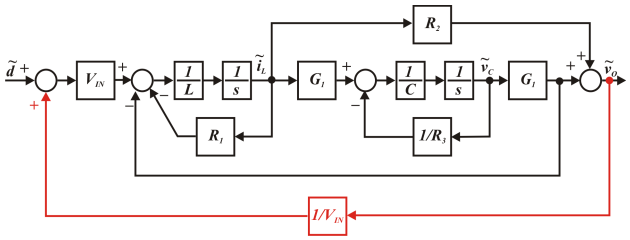

Fig. 5. Average state block diagram of buck converter

It is important to notice that even with the cross-coupling decoupling of Fig. 6 the use of just a PI controller does not improve the performance of the closed loop system. In general, just a PI controller for the output voltage results in complex closed loop poles. To solve this problem it is necessary to use cascade current and voltage controllers. Designing an inner current controller whose bandwidth is much larger (at least one decade) than the voltage one, the system bandwidth could be located wherever desired by defining the voltage outer loop bandwidth since the current block could be considered approximately ideal (unity gain system).

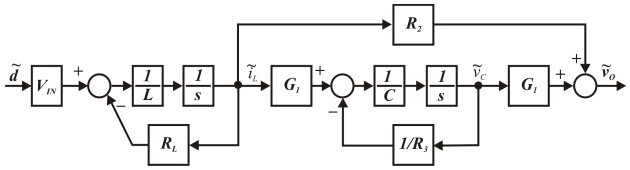

Fig. 6. Average block diagram of the decoupled Buck converter.

C. State Space Controller Serial Tuning

Because it is possible to analyze each state independently (after cross-coupling decoupling), the block diagram used to tune the inner current controller loop is showed in Fig. 7. As noted earlier,, a P controller can be used for this state. In this case, $G_c(s) = K_{pc}$. By defining this controller bandwidth as B_{wc} (Hz), the gain K_{pc} can be calculated as (21).

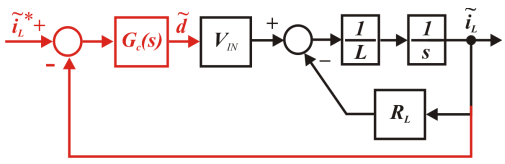

Fig. 7. Block diagram used to tune the current loop.

$$K_{pc} = \frac{2\pi B_{wv} L - R_L}{V_{IN}} \tag{21}$$

When the current inner loop is tuned for much higher bandwidth than the voltage outer loop, its dynamics are nearly independent of the voltage loop, making it possible to tune the voltage loop using the simplified state block diagram shown in Fig. 8. The current loop is approximated by a unity gain, and a PI voltage controller is used.

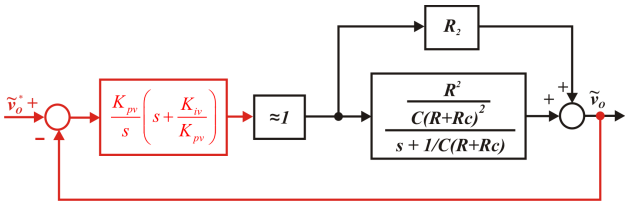

Fig. 8. Block diagram used for serial tuning of the voltage loop.

To design the voltage regulator, the PI controller zero (K_{iv}/K_{pv}) must be selected. One commonly used approach is to cancel the plant pole, in this case p_2. Using this choice and defining the voltage controller bandwidth as B_{wv} (Hz), the gains of this regulator are calculated using (22) and (23). The gain $z = \frac{1}{CR_C}$.

$$K_{pv} = \frac{2\pi B_{wv}}{R_2(z + B_{wv})} \tag{22}$$

$$K_{iv} = -K_{pv} p_2 \tag{23}$$

V. Simulation Results

In order to verify the performance of the state space controller proposed in this paper and compare to the k-factor approach, a set of simulation experiments were carried out using the buck converter with the parameters and specifications showed in Table V. In the case of the state space controller, the inner current loop bandwidth was set to *10 kHz*. The outer voltage loop bandwidth was set to *1 kHz* in both controllers. For the case of the k-factor the designed phase margin was $PM = 60^o$. The cross-coupling decoupling shown in Fig. 5 was done using the rated input voltage of 12 V. Several situations were simulated: 1) startup; 2) input voltage variation; 3) load voltage variation.

TABLE V
Parameters of the Buck Converter Used in The Simulation

Output voltage (v_o):	*5 V*
Ripple in v_o (Δv_o):	*50 mV (1 %)*
Input voltage (V_{IN}):	*9 V ≤ V_{IN} ≤ 15 V*
Ripple in i_L (Δi_L):	*20 %*
Rated output current (i_o):	*2 A*
Switching frequency (f_s):	*50 kHz*
Output Capacitor (C)	*188 μF*
Output Capacitor ESR (R_C):	*72 mΩ*
Inductor (L):	*150 μH*
Inductor ESR (R_L):	*85 mΩ*

Fig. 9 shows the startup comparison of the k-factor and state feedback design. The settling time t_s (within 2 % of the final value) of the state feedback design is approximately *400 µs* and *4.88 ms* for the k-factor design which is 12 times bigger. One of the reasons for this much longer settling time is the order of the controller (3rd order) whiles in the state feedback design the controller has dominant *1st* order dynamics.

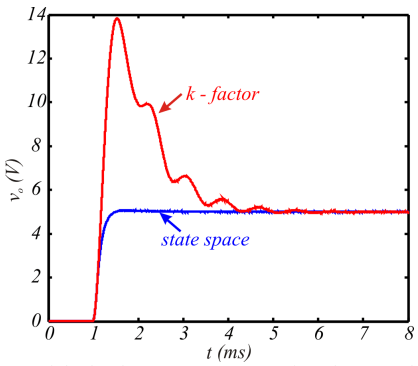

Fig. 9. Startup of the buck converter: comparison between k-factor and state space decoupling designs.

Fig. 10 shows the results for a step change in the input voltage. The step amplitude variation was ΔV_{IN} = - *25% (12 V → 9 V)* at t = *8 ms*, ΔV_{IN} = + *25% (9 V → 12 V)* at t = *16 ms*. The state space controller is practically insensitive to input voltage variations, despite the fact that the cross-coupling decoupling was done using the rated input voltage. This voltage is not measured, and therefore it cannot be dynamically updated in the analog circuitry used for the decoupling. On the other hand, the k-factor controller is very sensitive to input voltage variations showing an oscillatory behavior after the input voltage change. By comparison t_s = *0* for the state space controller because the voltage change was smaller than 2 % of the final value, and t_s = *2.2 ms* for the k-factor design to reach the same value.

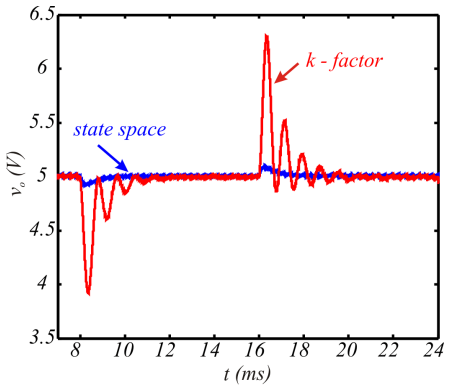

Fig. 10. Response to a step change in the input voltage (ΔV_{IN} = ± *33%*): comparison between k-factor and state space decoupling designs.

Fig. 11 shows the results for a step change in the load. The step amplitude variation was Δi_o = - *50 % (2 A → 1 A)* at t = *7 ms*, Δi_o = + *50 % (1 A → 2 A)* at t = *16 ms*. Again, the state space controller responds without oscillation and with t_s = *189 µs*. The k-fator controller exhibits oscillatory behavior with t_s =*2.36 ms*.

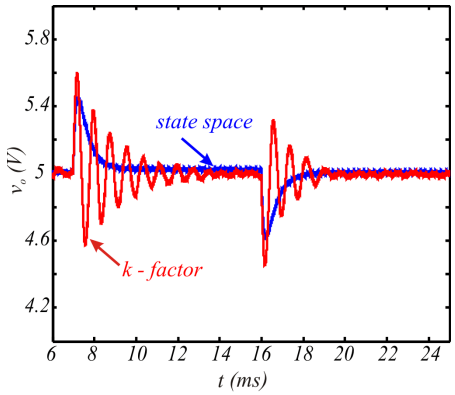

Fig. 11. Response to a step change in the load current (Δi_o = ± *50%*): comparison between k-factor and state space decoupling designs.

The simulation results showed that the proposed state space controller has the expected behavior. Because the current and voltage states were decoupled, it was possible to design the two loops to nearly independently control each state. A proportional controller was used for the inner current loop, and a PI controller for the voltage outer loop. The combination results in the system possessing dominant lower order dynamics than in the case of the k-factor design. Furthermore, the poles are located in the real axis for the state space controller, resulting in transient response without oscillation.

It should be noted that the k-factor controller only has an explicit loop on the output voltage, and the state space design explicitly has two loops. To make a fair comparison, the state space design should be compared to other techniques that implement two loops e.g. the ones presented in [5], [6]. There are two reasons why this type of comparison was not made in this paper: 1) the current controller bandwidth is not clear in those papers; 2) their implementation usually is much more complex than the state space design presented here. However, independently of the comparison, the design proposed in this paper exhibits very good dynamic properties.

VI. Experimental Results

The experimental results were carried out using a prototype with similar parameters to those used in the simulation. Except for the parasitic elements of the inductor, capacitor, MOSFET, and diode, the fundamental parameters were the same. However, the measured ESR of the inductor and capacitor, at *20 kHz*, were the same as those presented in Table V (R_L = 85 $m\Omega$ and R_C = 72 $m\Omega$). The LCR meter used for the measurements operates at specific frequencies, and 20 kHz was the closest to the switching frequency used in the circuit. Three tests were performed: 1) startup; 2) input voltage variation; 3) load variation.

The state space controller was implemented using the circuit showed in Fig. 12. The current measurement is based on a Hall effect sensor whose output is represented by v_I in Fig. 12. The measured voltage is represented by v_o and the reference voltage by v_o^*. The current loop bandwidth was set to *10 kHz*, and the voltage loop bandwidth was set to *1 kHz*. Using these bandwidths and

the circuit components presented in Table V, the controller parameters were calculated and are shown in Table VI. The resistors R_1, R_7, R_{11} and R_{16} are selected to reduce the effects of input bias current of the op-amps.

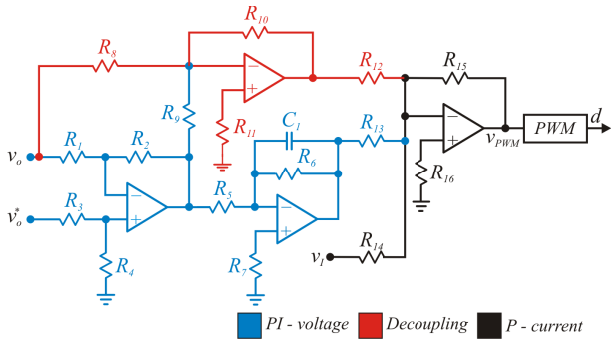

Fig. 12. State Space controller with cross-coupling decoupling.

TABLE VI
PARAMETERS OF THE STATE SPACE CONTROLLER AS IMPLEMENTED

$R_1 = R_2 = R_3 = R_4 = 40.2\ k\Omega$	$R_5 = R_7 = 27\ k\Omega$
$R_6 = 680\ k\Omega$; $R8 = 604\ k\Omega$	$R_9 = R_{13} = 41.2\ k\Omega$
$R_{10} = R_{12} = R_{15} = 100\ k\Omega$	$R_{11} = R_{16} = 9.3\ k\Omega$
$R_{14} = 68{,}1\ k\Omega$	$C_1 = 20nF$

Fig. 13 shows the experimental results during startup of the buck converter. Both figures present the reference (green) and the output voltage (orange). Fig. 13a shows the results for the state space controller and Fig. 13b shows the results for the k-factor controller. For the case of the k-factor design, the bandwidth and phase margin were $1\ kHz$ and $PM = 60^o$, respectively. The first conclusion is that the behavior of both controllers is similar to the simulation results, the state space design having a $t_s \cong 320\ \mu s$ and the k-factor design a $t_s \cong 5\ ms$ with an overshoot of more than 100%.

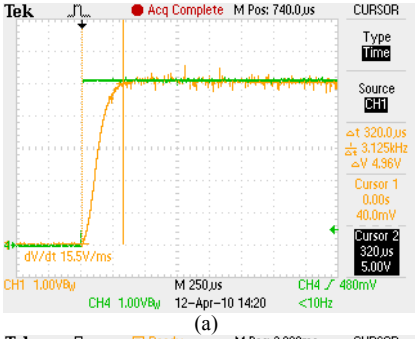

(a)

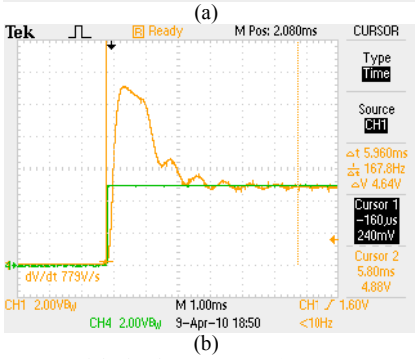

(b)

Fig. 13. Startup of the buck converter: (a) state space controller; (b) k-factor controller. CH1 – output voltage; CH4 – reference voltage.

Fig. 14 shows the experimental results for a step change in the input voltage. Both figures present the output voltage (CH1) and input voltage (CH2). The noise shown in the input voltage is due to removal of the input filter of the converter. This was necessary to experimentally implement the step change in the input voltage . Otherwise this type of variation would not be possible. The step amplitude variation was $\Delta V_{IN} = +\ 25\%\ (12\ V \rightarrow 15\ V)$. Similar to the simulation results, the state space controller is almost insensitive to input voltage variations. For the case of k-factor controller the output voltage variation was oscillatory with an overshoot of $16\ \%$ and $t_s \cong 6\ ms$.

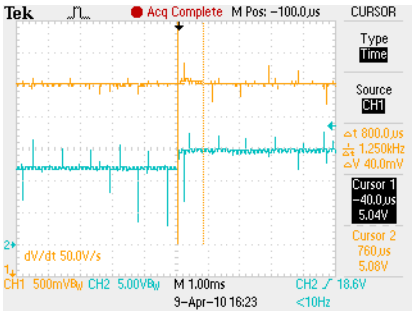

(a)

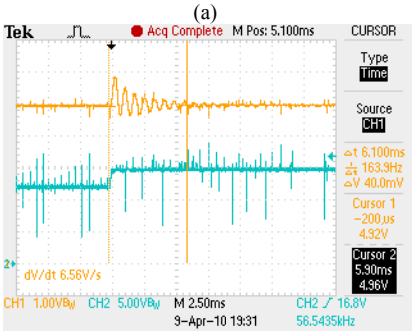

(b)

Fig. 14. Response to a step change in the input voltage ($\Delta V_{IN} = +\ 33\%$): (a) state space controller; (b) k-factor controller. CH1 – output voltage; CH2 – input voltage.

Fig. 15 shows the experimental results for a 50% step change in the load current. The load variation was implemented by switching another resistor in parallel with the load. Both figures present the output voltage (CH1) and output current (CH2). The behavior of both controllers is similar to that of the simulation results, the state space controller having better disturbance rejection properties than the k-factor design. The settling time was $t_s \cong 750\ \mu s$ for the state space controller, and $t_s \cong 2.5\ ms$ for the k-factor controller.

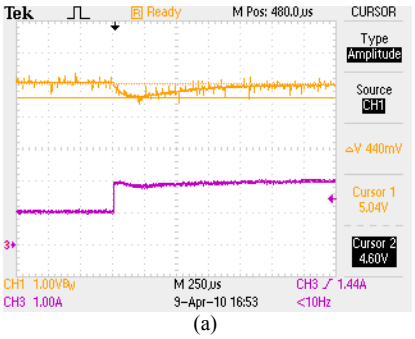

(a)

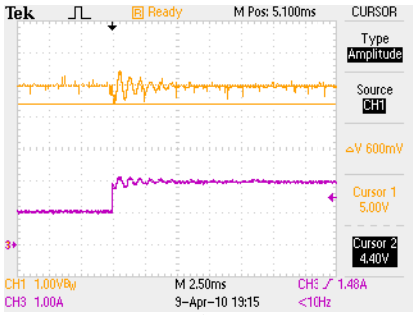

(b)

Fig. 15. Response to a step change in the load current ($\Delta i_o = +50\%$): comparison between (a) state space controller, and (b) k-factor controller. CH1 – output voltage; CH3 – output current

VII. Conclusions

In this paper, a state space decoupling control technique for dc-dc converters was presented, which was compared to the k-factor design approach. Using small signal analysis, the equations of the converters were obtained. With the state space average differential equations of the converter, the average model, state block diagrams were developed. These block diagrams show, in a global manner, how the state variables (capacitor voltage and inductor current) are cross-coupled and how it is possible to decouple the interaction between states. State space cross-coupling decoupling was applied to a buck converter, resulting in a system with real poles. With these pole locations and the decoupled cross-coupling, the controller design for the voltage and current loops were nearly independent. Simulation and experimental results showed that the state space controller response possessed good immunity to input voltage variation, a faster transient response with lower overshoot and no oscillation when compared to the k-factor controller. The results suggest that the state space controller with cross-coupling decoupling can be applied to other converters as well.

Acknowledgment

The authors would like to acknowledge the financial support and motivational provided by the Ministry of Mines and Energy, CNPq, the Federal University of Maranhão (UFMA), and Texas Instruments.

References

[1] G.W.Wester and R.D.Middlebrooks, "Low-Frequency Characterization of switched Dc-Dc Converters", IEEE Transactions on Aerospace and electronic Systems, Vol. AES-9, pp. 376-385, May 1973.

[2] V. Vorperian, "Simplified Analysis of PWM Converters Using the Model of the PWM Switch: Parts I and II", IEEE Transaction on Aerospace and electronic Systems, Vol. AES-26, pp.490-505, May 1990.

[3] N. Mohan, T.M. Underland, W.P. Robbins, "Power Electronics: Converters, Applications and design, Third Edition", John Wiley, 2002.

[4] L. H. Dixon, "Average current-mode control of switching power supplies", in *Unitrode Power Supply Design Seminar Handbook*, 1990.

[5] B. Bryant, M.K.Kazimierczu,"Modeling the Closed-Current Loop of PWM Boost DC-DC Converters Operating in CCM with Peak Current-Mode Control". IEEE Transactions on Circuits and Systems. Vol. 52, Nº 11. pp. 2404-2412. 2005.

[6] G. Gabriel, M. Pascual. E. Figueres, "Robust Average Current-Mode Control of Multimodule Parallel DC-DC PWM Converter Systems with Improved Dynamic Respnse". IEEE Transactions on Industrial Electronics. Vol. 48, Nº 5. pp. 995-1005. 2001.

[7] H. D. venable, "The k-factor: A mathematical Tool for Stability, Analysis and Synthesis", *Proceeding of Powercon 10*, San Diego, CA, March 22-24, 1983.

[8] R. D. Lorenz, D. B. Lawson. Performance of Feedforward Current Regulators for Field-Oriented Induction machine Controllers". *IEEE Transactions on Industry Applications*, Vol. IA-23, No. 4, July/August 1987.

[9] M. J. Ryan, W. E. Brumsickle, and R. D. Lorenz, "Control Topology Options for Single Phase UPS Inverters", IEEE Trans. on Ind. Appl., Vol 33, No.2, March/April 1997, pp.493-501.

[10] E. C. Gomes, L. A. S. Ribeiro, S. Y. C Catunda. "State Space Control for Buck Converter Using Decoupled Block Diagram Approach". *Procedings of 10th Brazilian Power Electronics Conference*. *Bonito-Brazil*. pp.686-693. 2009.